

Cascade control of the moto-compressor of a PEM fuel cell via second order sliding mode

Imad Matraji, Salah Laghrouche and Maxime Wack
 Laboratoire S.E.T, Universite de Technologie de Belfort-Montbéliard, Belfort, France.

imad.matraji@utbm.fr, salah.laghrouche@utbm.fr, maxime.wack@utbm.fr

Abstract—This paper presents a cascade control of the moto-compressor of a Polymer Electrolyte Membrane Fuel Cell (PEMFC). The control objective is to optimize the net power by maintaining the oxygen excess ratio between 2 and 2.4. The proposed control strategy is based on two cascaded super twisting second order sliding mode controllers (Fig.1), which regulate the moto-compressor supplying air to the cathode side of the fuel cell. Simulation results show that the proposed controller has a good transient performance under load variations and parametric uncertainties.

I. INTRODUCTION

The main problem of a fuel cell is oxygen starvation when the load changes rapidly. If the load increases, it needs more power and the current of the fuel cell increases. The chemical reactions need to be accelerated to provide the required power to the load, using more oxygen. Hence precise control of moto-compressor, which supplies air to the fuel cell, is important in order to optimize the net output power. In the last few years, many control strategies have been proposed for control of the moto-compressor of the PEMFCs, notable among them are linearizing at an operating point with a feedforward and feedback control [1], neural networks [2], model predictive control [3], [4] and sliding mode control [5], [6], [7].

In this paper we have proposed a cascade control strategy using second order sliding mode control (SOSMC) for PEMFC, using super twisting algorithm. The proposed control law is based on the works of [8] and [9], which have been developed to counteract the chattering phenomenon while preserving the main advantages of standard sliding mode control. The control objective is to maintain the oxygen excess ratio $\lambda_{O_2} = 2$ because the highest net power P_{net} is achieved at an oxygen excess ratio between 2 and 2.4. The proposed cascade controller contains two loops. The outer loop performs a feedback-linearized SOSMC of the oxygen excess ratio, generating the reference compressor air flow for the inner loop. The inner loop controls the moto-compressor (voltage) using a second SOSMC and feedback linearization (FBL). Fig.1 In order to synthesize a good control law, a comprehensive dynamic model is required. The most detailed model that exists in the literature is the 9 state model proposed by Pukrushpan [1].

$$x = [m_{O_2}, m_{H_2}, m_{N_2}, \omega_{cp}, p_{sm}, m_{sm}, m_{w,an}, m_{w,ca}, p_{rm}]^T$$

where m_{O_2} , m_{H_2} and m_{N_2} are the mass of oxygen, hydrogen and nitrogen, respectively, ω_{cp} is the compressor speed,

p_{sm} and m_{sm} are the pressure and the mass of the supply manifold, respectively, $m_{w,an}$ and $m_{w,ca}$ are the mass of water in the anode and the cathode side, respectively and p_{rm} is the pressure of the return manifold. The number of states however, restricts its use in control applications, due to the large number of calculations required. In our study, we have considered reduced forms of Pukrushpan's model. Two reduced forms of the this model exist in contemporary literature. The first form has been proposed in [10]. It reduces the model to 4 states under the following five assumptions:

- 1) The water mass in the anode and the cathode side will be constant, they are equal to the maximum vapor mass because the gas is humidified at $100^\circ C$ or saturated, in the cathode and the anode side.
- 2) The control of the hydrogen is ensured by an electrovalve which has faster dynamics than the dynamics of the air circuit of the moto compressor. The anode pressure input is hence regulated as a function of the cathode pressure input or the compressor mass flow rate. The pressure of the anode side will therefore be equal to the pressure of the cathode side.
- 3) The supply manifold mass will be proportional to the manifold pressure, since the gas in the supply manifold verifies the properties of the ideal gas.
- 4) The return manifold pressure is equal to the atmospheric pressure as the pressure drop across the manifold is negligible because the volume of the return manifold is negligible.
- 5) All the gases are ideal so the masses of oxygen and nitrogen gases can be replaced by their partial pressures.

The second reduced form, proposed in [11], reduces the model to 3 states under two further assumptions:

- 1) The entire cathode pressure is considered as a state, instead of considering nitrogen and oxygen pressures individually. Moreover, the individual molar masses of oxygen, nitrogen and water are assumed to have the same magnitude, and are replaced by a single constant.
- 2) The cathode exit flow rate is assumed as critical flow or choked flow.

Our controller has been designed around the 3-state model. This paper has been divided as follows. The mathematical model of the PEMFC dynamics has been described in Section 2. In section 3 we present the system measurement and performance of the PEMFC. In section 4 the method of second order sliding mode control has been detailed. Section 5 presents the control design of the controller proposed. Section 6 presents the simulation results. Finally, conclusion

are presented in section 7.

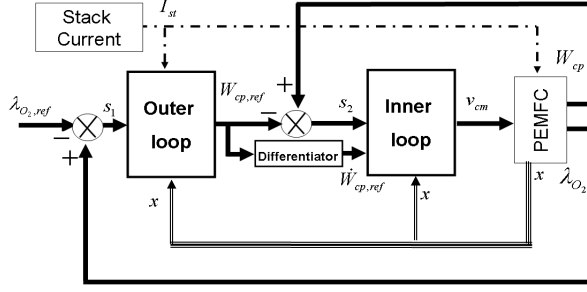


Fig. 1. Proposed cascaded control structure

II. DYNAMIC MODEL

In this section we present the nonlinear dynamic model of the fuel cell system proposed in [11]. This model has 3 states, which are:

$$x = [p_{ca}, \omega_{cp}, p_{sm}]^T$$

where p_{ca} is the cathode pressure in Pascal (Pa), ω_{cp} is the compressor speed in radian per second (rad/s) and p_{sm} is the supply manifold pressure in Pascal (Pa).

According to the ideal gas law and the mass conservation rule:

$$\frac{dp_{ca}}{dt} = \frac{T_{fc}}{V_{ca}} \left(\frac{R}{M_a} W_{ca,in} - \frac{R}{\kappa} W_{ca,out} - \frac{R}{M_{O_2}} W_{ca,reacted} \right) \quad (1)$$

where R is the universal gas constant, M_a and M_{O_2} are the molar masses of air and oxygen respectively, κ is the constant mentioned in the assumption 1 by [11]. V_{ca} is the cathode volume, $W_{ca,in}$ is the inlet cathode mass flow rate, $W_{ca,out}$ is the outlet cathode mass flow rate and $W_{ca,reacted}$ is the reacted mass flow rate in the cathode. $W_{ca,in}$ is expressed as follows:

$$W_{ca,in} = \frac{1}{1 + \omega_{atm}} W_{in} \quad (2)$$

$$\text{with } \omega_{atm} = \frac{M_v}{M_a} \frac{\phi_{atm} p_{sat}(T_{atm})}{p_{atm} - \phi_{atm} p_{sat}(T_{atm})}$$

$$W_{in} = k_{ca,in} (p_{sm} - p_{ca})$$

where M_v is the molar mass of vapor, ϕ_{atm} is the relative humidity at ambient conditions (preset to the average value 0.5), $p_{sat}(T_{atm})$ is the saturation pressure at the ambience temperature, p_{atm} is the atmospheric pressure and $k_{ca,in}$ is the cathode inlet orifice constant. $W_{ca,out}$ is expressed as follows:

$$W_{ca,out} = \frac{p_{ca} - p_{sat}(T_{fc})}{p_{ca}} W_{out} \quad (3)$$

As W_{out} is assumed to be choked flow [11] ($\frac{p_{atm}}{p_{ca}} \leq \left(\frac{2}{\gamma+1}\right)^{\frac{\gamma}{\gamma-1}}$), we obtain

$$W_{out} = \frac{C_D A_T p_{ca}}{\sqrt{RT_{fc}}} \frac{1}{\gamma^2} \left(\frac{2}{\gamma+1}\right)^{\frac{\gamma+1}{2(\gamma-1)}} \quad (4)$$

where γ is the specific heat ratio of air, C_D is the discharge constant of the nozzle and A_T is the opening area of the nozzle. The saturation pressure is calculated as a function of the fuel cell temperature T_{fc} , and it is presented as follows:

$$\log_{10}(p_{sat}(T_{fc})) = (-1.69 * 10^{-10} T_{fc}^4 + 3.85 * 10^{-7} T_{fc}^3 - 3.39 * 10^{-4} T_{fc}^2 + 0.143 T_{fc} - 20.92) * 10^3 \quad (5)$$

Oxygen is the only gas which reacts on the cathode side. Electrochemistry principles are used to calculate the rate of oxygen consumption. The mass flow rate of oxygen reacted in the cathode $W_{ca,reacted}$ is expressed as follows:

$$W_{ca,reacted} = M_{O_2} \frac{n I_{st}}{4F} \quad (6)$$

where, n is the number of cells in the stack, F is the faraday number and I_{st} is the stack current.

The angular speed ω_{cp} verifies the following differential equation:

$$\frac{d\omega_{cp}}{dt} = \frac{1}{J_{cp}} (\tau_{cm} - \tau_{cp}) \quad (7)$$

where, J_{cp} is the compressor motor inertia. τ_{cm} and τ_{cp} denote the compressor motor torque and the load torque required to drive the compressor respectively.

$$\tau_{cm} = \frac{k_t \eta_{cm}}{R_{cm}} (v_{cm} - k_v \omega_{cp})$$

$$\tau_{cp} = \frac{C_p T_{atm}}{\eta_{cp} \omega_{cp}} \left[\left(\frac{p_{sm}}{p_{atm}} \right)^{\frac{\gamma-1}{\gamma}} - 1 \right] W_{cp} \quad (8)$$

where R_{cm} , k_t and k_v are motor constants, η_{cp} is the compressor efficiency, η_{cm} is the motor mechanical efficiency, C_p is the specific heat capacity of air, v_{cm} is the compressor motor voltage and W_{cp} is the compressor mass flow rate (expressed in equation (15)).

The air pressure in the supply manifold is given by the following differential equation:

$$\frac{dp_{sm}}{dt} = \frac{RT_{cp}}{M_a V_{sm}} (W_{cp} - W_{in}) \quad (9)$$

where, V_{sm} is the supply manifold volume and T_{cp} is the temperature leaving the compressor.

$$T_{cp} = T_{atm} + \frac{T_{atm}}{\eta_{cp}} \left[\left(\frac{p_{sm}}{p_{atm}} \right)^{\frac{\gamma-1}{\gamma}} - 1 \right] \quad (10)$$

The model can be written as follows:

$$\dot{x} = f(x) + g_u u + g_\xi \xi$$

$$x = \begin{bmatrix} x_1 := p_{ca} \\ x_2 := \omega_{cp} \\ x_3 := p_{sm} \end{bmatrix} ; \quad u := v_{cm} ; \quad \xi := I_{st} \quad (11)$$

Where the control input u is the compressor motor voltage, the input ξ is the stack current and is considered as measurable disturbance to the system.

III. SYSTEM MEASUREMENT AND PERFORMANCE

A. System measurement

The system measurement or output is defined by:

$$y = \begin{bmatrix} V_{st} \\ p_{sm} \\ W_{cp} \end{bmatrix} \quad (12)$$

where V_{st} , p_{sm} and W_{cp} are the stack voltage, the supply manifold pressure and the compressor air flow, respectively. The stack voltage (13) is the sum of the voltages of elementary cells, connected in series.

$$V_{st} = nV_{fc} \quad (13)$$

The fuel cell voltage (14) is defined as a function of the current density, saturation pressure, partial pressures of oxygen and hydrogen, fuel cell temperature and membrane humidity [12][1].

$$V_{fc} = E - V_{activation} - V_{ohmic} - V_{concentration} \quad (14)$$

The voltage E is called the reversible open circuit voltage or the "Nernst" voltage of a hydrogen fuel cell. The activation loss $V_{activation}$ is due to the chemical reactions and the electron movement between the anode and the cathode. Ohmic losses V_{ohmic} occur due to two main causes, the resistance of the polymer membrane to the transfer of protons, and the resistance of both the electrodes and the collector plate to the transfer of electrons. The concentration loss $V_{concentration}$ or concentration over-voltage results from the concentration drop of the reactants as they are consumed in the reaction [13].

The air flow at the output of the compressor is a function of the angular speed of the moto-compressor and the supply manifold pressure. It can be written as follows [7]:

$$W_{cp} = k_{15} \left[1 - e^{-k_{16} \left(\left(\frac{p_{sm}}{p_{atm}} \right)^{k_{17}} - 1 \right) \omega_{cp}^{-2} - k_{18}} \right] \omega_{cp} \quad (15)$$

where the constants k_{15} , k_{16} , k_{17} and k_{18} are defined in appendix [A].

B. System performance

The system performance is defined by:

$$z = \begin{bmatrix} P_{net} \\ \lambda_{O_2} \end{bmatrix} \quad (16)$$

Where P_{net} and λ_{O_2} are the net power and the oxygen excess ratio, respectively. The net power P_{net} of the fuel cell system is the difference between the power produced by the stack and the compressor motor power. For certain stack currents, stack voltage increases with increasing air flow rate to the stack because the cathode oxygen partial pressure increases. The excess amount of air flow provided to the stack is normally indicated by the term oxygen excess ratio λ_{O_2} , defined as the ratio of oxygen supplied and oxygen used in the cathode.

The two performance parameters are calculated as follows:

$$\begin{aligned} P_{net} &= P_{st} - P_{cm} \\ \lambda_{O_2} &= \frac{W_{O_2,in}}{W_{O_2,react}} \end{aligned} \quad (17)$$

where

$$\begin{aligned} P_{st} &= V_{st} I_{st} \\ P_{cm} &= \frac{v_{cm}}{R_{cm}} (v_{cm} - k_v \omega_{cp}) \\ W_{O_2,in} &= x_{O_2,ca,in} W_{ca,in} \\ W_{O_2,react} &= W_{ca,reacted} \end{aligned} \quad (18)$$

$$\text{with } x_{O_2,ca,in} = \frac{y_{O_2,ca,in} M_{O_2}}{y_{O_2,ca,in} M_{O_2} + (1 - y_{O_2,ca,in}) M_{N_2}}$$

where $y_{O_2,ca,in}$ is the oxygen mole fraction and M_{N_2} is the nitrogen molar mass.

IV. SECOND ORDER SLIDING MODE

Consider a single-input nonlinear system

$$\begin{aligned} \dot{x} &= f(x) + g(x)u \\ y &= s(x) \end{aligned} \quad (19)$$

with $x \in \mathcal{X} \subset \mathbb{R}^n$ the state variable and $u \in \mathcal{U} \subset \mathbb{R}$ the input, such that $\mathcal{X} = \{x \in \mathbb{R}^n \mid |x_i| \leq x_{iMAX}, 1 \leq i \leq n\}$ and $\mathcal{U} = \{u \in \mathbb{R} \mid |u| \leq u_{MAX}\}$. f and g are smooth uncertain functions.

Suppose that the control objective is to force a defined output function (called sliding variable) $s(x)$ to zero. The relative degree of the system is assumed to be constant and known. We suppose that the control explicitly appears in the 1st time derivative of s

$$\dot{s} = \frac{\partial}{\partial x} [s] [f(x) + g(x)u] \quad (20)$$

There exist positive constant values C , K_m and K_M so that, $\forall u \in \mathcal{U}$ and $\forall x \in \mathcal{X}$,

$$0 < K_m < \frac{\partial}{\partial u} \dot{s} < K_M, \quad \left| \frac{\partial}{\partial x} \dot{s} \right| \leq C \quad (21)$$

Consider local coordinates $[\zeta_1 \ \zeta_2]^T = [s \ \dot{s}]^T$. Then, on the basis of the previous definitions and conditions, the second order sliding mode problem becomes the finite time stabilization problem of the following uncertain second order system [9], [14]

$$\begin{cases} \dot{\zeta}_1 = \zeta_2 \\ \dot{\zeta}_2 = a(x) + b(x)v \end{cases} \quad (22)$$

where ζ_2 may be unmeasurable. Referring to the previous notation, $v = u$ is the control input. There are several algorithms which ensure the finite time stabilization of the system (22) towards the origin [9], [15]. Among them, the so-called "Super Twisting algorithm" relies on inserting an integrator into the controller loop, such that control becomes a continuous time function. This algorithm is defined by the following control law [9], [15]

$$\begin{aligned} u &= u_1 + u_2 \\ \dot{u}_1 &= -\beta_s \text{sign}(s) \\ u_2 &= -\alpha_s |s|^{\frac{1}{2}} \text{sign}(s) \\ \alpha_s > 0 &; \beta_s > 0 \end{aligned} \quad (23)$$

with the following sufficient conditions which ensure the finite time convergence to the sliding manifold.

$$\beta_s > \frac{C}{K_m}, \quad \alpha_s^2 \geq \frac{4CK_M(\beta_s + C)}{K_m^3(\beta_s - C)} \quad (24)$$

V. CONTROL DESIGN

The dynamical equations of the simplified model can be presented as follows :

$$\begin{aligned} \dot{x}_1 &= k_1 x_3 - (k_1 + k_2)x_1 + k_3 - k_4 \xi \\ \dot{x}_2 &= -k_5 x_2 - \frac{k_6}{x_2} \left[\left(\frac{x_3}{k_7} \right)^{k_8} - 1 \right] W_{cp} + k_9 u \\ \dot{x}_3 &= k_{10} \left[1 + k_{11} \left[\left(\frac{x_3}{k_7} \right)^{k_8} - 1 \right] \right] [W_{cp} - k_{12}(x_3 - x_1)] \end{aligned} \quad (25)$$

$$x = \begin{bmatrix} x_1 \\ x_2 \\ x_3 \end{bmatrix} ; \quad u = v_{cm} ; \quad \xi = I_{st} \quad (26)$$

where the constants $k_1, k_2 \dots$ and k_{12} are defined in appendix [A].

Second order sliding mode control (2-SMC) technique [8], [16] is used to design a cascade-based architecture, represented by the block diagram in Fig.1. This control method is known to be robust against disturbances and parametric uncertainties. The control objective is to maintain the oxygen excess ratio on 2. The controller system is decomposed into 2 parts the outer loop and the inner loop. The outer loop, "2-SMC oxygen excess ratio controller", contains the Super Twisting algorithm, with the oxygen excess ratio error as input. The output of the controller $W_{cp,ref}$ is the reference compressor air flow. This serves as the reference for the inner loop, "compressor air flow controller" which produces the compressor motor voltage v_{cm} to be applied to the PEMFC. The detailed scheme of the controller is presented in the Fig.2. Two sliding manifolds have been chosen to force λ_{O_2} and W_{cp} towards the equilibrium points $\lambda_{O_2,ref}$ and $W_{cp,ref}$ respectively, the manifolds are defined for the outer and inner loops.

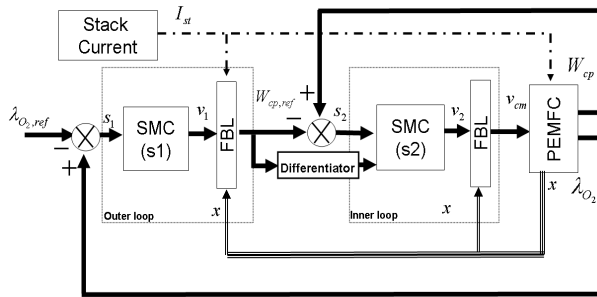


Fig. 2. Detailed diagram of the proposed control system

A. Outer loop

The manifold of the outer loop is defined as:

$$\begin{aligned} s_1 &= \lambda_{O_2} - \lambda_{O_2,ref} \\ s_1 &= \frac{k_{13}}{k_{14}I_{st}}(x_3 - x_1) - \lambda_{O_2,ref} \end{aligned} \quad (27)$$

Consider the first time derivative of s_1

$$\begin{aligned} \dot{s}_1 &= \dot{\lambda}_{O_2} - \dot{\lambda}_{O_2,ref} \\ \dot{s}_1 &= \frac{k_{13}}{k_{14}I_{st}} \left(k_{10} \left[1 + k_{11} \left[\left(\frac{x_3}{k_7} \right)^{k_8} - 1 \right] \right] \right. \\ &\quad \left. [W_{cp,ref} - k_{12}(x_3 - x_1)] - (k_1 x_3 - (k_1 + k_2)x_1 \right. \\ &\quad \left. + k_3 - k_4 I_{st}) \right) \end{aligned} \quad (28)$$

where the constants k_{13} and k_{14} are defined in appendix [A]. Using feedback linearization technique,

$$W_{cp,ref} = \gamma_1(t, x)^{-1}(v_1 - \phi_1(t, x)) \quad (29)$$

with

$$\begin{aligned} \phi_1(t, x) &= \frac{k_{13}}{k_{14}I_{st}} \left(k_{10} \left[1 + k_{11} \left[\left(\frac{x_3}{k_7} \right)^{k_8} - 1 \right] \right] \right. \\ &\quad \left. * (-k_{12}(x_3 - x_1) - (k_1 x_3 - (k_1 + k_2)x_1 \right. \right. \\ &\quad \left. \left. + k_3 - k_4 I_{st}) \right) \right) \end{aligned} \quad (30)$$

$$\gamma_1(t, x) = \frac{k_{13}k_{10}}{k_{14}I_{st}} \left[1 + k_{11} \left[\left(\frac{x_3}{k_7} \right)^{k_8} - 1 \right] \right]$$

where v_1 leads to one integrator $\dot{s}_1 = v_1$ and is designed to stabilize this new system:

$$\begin{aligned} v_1 &= v_{11} + v_{12} \\ \dot{v}_{11} &= -\beta_1 \text{sign}(s_1) \\ v_{12} &= -\alpha_1 |s_1|^{\frac{1}{2}} \text{sign}(s_1) \\ \alpha_1 = 3 &; \quad \beta_1 = 0.5 \end{aligned} \quad (31)$$

α_1 and β_1 respect the conditions given in equation (24).

B. Inner loop

The manifold of the inner loop is defined as:

$$s_2 = W_{cp} - W_{cp,ref} \quad (32)$$

Consider the first time derivative of s_2

$$\begin{aligned} \dot{s}_2 &= \dot{W}_{cp} - \dot{W}_{cp,ref} \\ \dot{s}_2 &= \phi_2(t, x) + \gamma_2(t, x)v_{cm} - \dot{W}_{cp,ref} \end{aligned} \quad (33)$$

with

$$\begin{aligned} \phi_2(t, x) &= \frac{\partial s}{\partial x_2} \dot{x}_2 + \frac{\partial s}{\partial x_3} \dot{x}_3 \\ \gamma_2(t, x) &= \frac{\partial s}{\partial v_{cm}} \end{aligned} \quad (34)$$

Using feedback linearization technique,

$$v_{cm} = \gamma_2(t, x)^{-1}(v_2 - \phi_2(t, x) + \dot{W}_{cp,ref}) \quad (35)$$

where v_2 leads to one integrator $\dot{s}_2 = v_2$ and is designed to stabilize this new system:

$$\begin{aligned} v_2 &= v_{21} + v_{22} \\ \dot{v}_{21} &= -\beta_2 \text{sign}(s_2) \\ v_{22} &= -\alpha_2 |s_2|^{\frac{1}{2}} \text{sign}(s_2) \\ \alpha_2 = 3 &; \quad \beta_2 = 2 \end{aligned} \quad (36)$$

α_2 and β_2 respect the conditions given in equation (24). In addition to the controller, a real time robust exact differentiator has been added [17] to obtain an exact derivative of $W_{cp,ref}$. The differentiator has the form:

$$\begin{cases} \dot{z}_0 = -\gamma_2 L^{\frac{1}{2}} |z_0 - s|^{\frac{1}{2}} \text{sign}(z_0 - s) + z_1 \\ \dot{z}_1 = -\gamma_1 L \text{sign}(z_1 - \dot{z}_0) \end{cases} \quad (37)$$

Where z_0 and z_1 are the real time estimations of $W_{cp,ref}$ and $\dot{W}_{cp,ref}$, respectively. The parameters of the differentiator γ_i are to be chosen empirically, in advance. $\gamma_1 = 1.1$, $\gamma_2 = 1.5$ have been suggested in [17]. L is the only differentiator parameter to be tuned, and it has to satisfy only one condition $|\dot{W}_{cp,ref}| \leq L$.

VI. MODEL VALIDATION AND SIMULATION RESULTS

The proposed control method has been simulated in the Matlab-Simulink environment. The stack current applied to the system has been chosen following [11]. It consists of rapid variations between 100 and 250 Amperes. The associated stack voltage varies between 225 and 260 Volts. The stack current and the stack voltage are presented in the Fig.3. The control objective of the cascade controller using second order sliding mode control is to stabilize the oxygen excess ratio on 2. During a positive current step transition (for example at $t = 6s$), the oxygen excess ratio drops as shown in Fig.4, and this causes a drop in the stack voltage as shown in Fig.3. We can remark that the controller ensures a rapid convergence of the oxygen excess ratio with an acceptable control input or compressor motor voltage as shown in the Fig.5. The compressor voltage varies between 0 and 200 Volts. Also, we avoid a $\lambda_{O_2} < 1$ during the load variations as it can cause irreversible damage to the PEMFC. The net power obtained from this controller is presented in the Fig.6. It can be seen that it varies between 20 and 50 kiloWatts. The compressor speed and the air flow are plotted in the Fig.7. Finally, the cathode pressure which varies between 1 and 2.4 bar and the supply manifold pressure which varies between 1.4 and 2.6 bar are plotted in Fig.8. Moreover, some parameters have been considered as uncertain (cited in Table.I). Fig.9 shows that the controller is robust under parametric uncertainties, the red line depicts the system trajectory in presence of uncertainties, while the blue dashed line shows the behavior of the undisturbed system. Fig.10 shows the difference in control curves between undisturbed system and uncertainties system. It can be concluded from these results that the proposed controller maintains its performance under load variations and uncertainties.

VII. CONCLUSION

In this paper, a nonlinear cascade control has been designed to regulate the oxygen excess ratio in a PEMFC, using super twisting second order sliding mode control. The control objective is to stabilize the oxygen excess ratio in order to get the highest net power. The PEMFC has been modeled using a reduced state model, subject to parametric uncertainty and load variations. The Simulations results obtained using Matlab-Simulink have shown that the cascade controller is

robust and has a good performance under load variations and uncertainties.

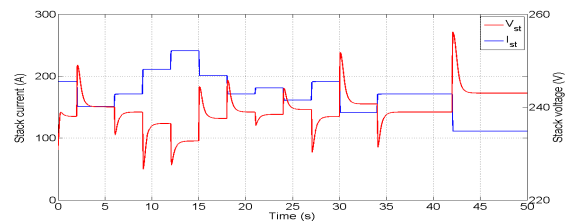


Fig. 3. Stack current and stack voltage under load variation

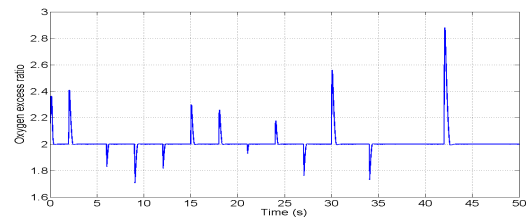


Fig. 4. Oxygen excess ratio

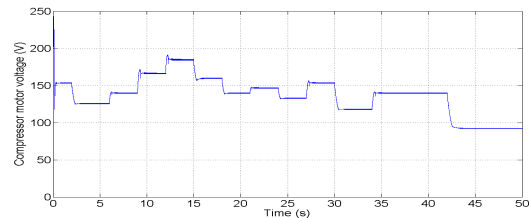


Fig. 5. Compressor motor voltage

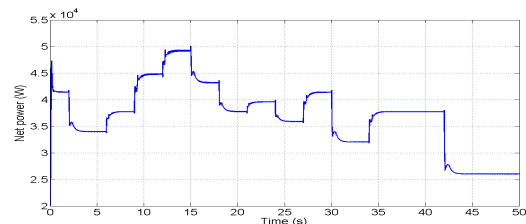


Fig. 6. Net power

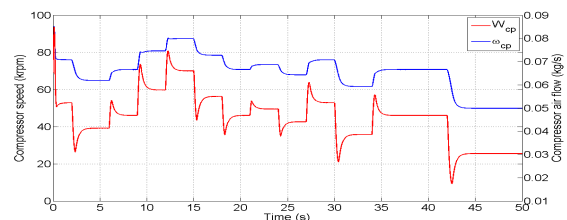


Fig. 7. Compressor speed and Compressor air flow

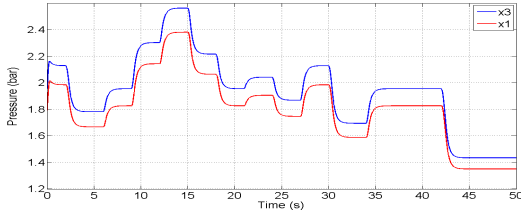


Fig. 8. Supply manifold and cathode pressures

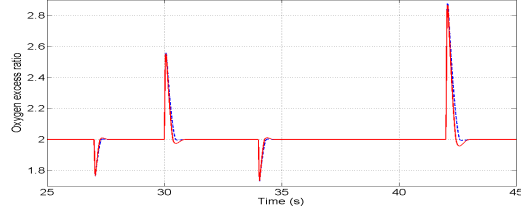


Fig. 9. Oxygen excess ratio under uncertainties variations

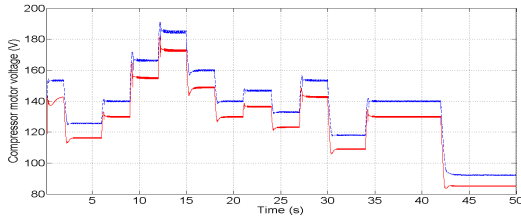


Fig. 10. Compressor motor voltage under uncertainties variations

A. Appendix

$$\begin{aligned}
 k_1 &= \frac{RT_{fc}k_{ca,in}}{V_{ca}M_a(1 + \omega_{atm})} \\
 k_2 &= \frac{RT_{fc}}{V_{ca}\kappa} \frac{C_D A_T}{\sqrt{RT_{fc}}} \gamma^2 \left(\frac{2}{\gamma+1} \right)^{\frac{\gamma+1}{2(\gamma-1)}} \\
 k_{15} &= \frac{\phi_{max}\rho_a\pi d_c^2 K_{U_c} \delta}{4\sqrt{\theta}} \\
 k_{13} &= k_{ca,in} \frac{x_{O_2,ca,in}}{1 + \omega_{atm}} \\
 k_3 &= k_2 p_{sat} \quad ; \quad k_4 = \frac{RT_{fc}n}{V_{ca}4F} \quad ; \quad k_5 = \frac{\eta_{cm}k_t k_v}{J_{cp}R_{cm}} \\
 k_6 &= \frac{C_p T_{atm}}{J_{cp}\eta_{cp}} \quad ; \quad k_7 = p_{atm} \quad ; \quad k_8 = \frac{\gamma-1}{\gamma} \\
 k_9 &= \frac{\eta_{cm}k_t}{J_{cp}R_{cm}} \quad ; \quad k_{10} = \frac{RT_{atm}}{M_a V_{sm}} \quad ; \quad k_{11} = \frac{1}{\eta_{cp}d_c} \\
 k_{12} &= k_{ca,in} \quad ; \quad k_{14} = \frac{nM_{O_2}}{4F} \quad ; \quad K_{U_c} = \frac{2\sqrt{\theta}}{2\sqrt{\theta}} \\
 k_{16} &= \frac{2\beta C_p T_{atm}}{\Phi_{max}K_{U_c}^2} \quad ; \quad k_{17} = \frac{\gamma-1}{\gamma} \quad ; \quad k_{18} = \beta
 \end{aligned}$$

REFERENCES

[1] J Pukrushpan, A Stefanopoulou, and H Peng. *Control of Fuel Cell Power Systems: Principles, Modeling and Analysis and Feedback Design*. Springer, 2004.

TABLE I

VARIATIONS OF PARAMETRIC UNCERTAINTIES

Parameter	Variation
Stack temperature (T_{st})	+10%
Cathode volume (V_{ca})	+5%
Motor constant (k_v)	-10%
Electric resistance of the motor (R_{cm})	+5%
Compressor diameter (d_c)	+1%
Motor inertia (J_{cp})	+10%

- [2] P Almeida and M G Simoes. Neural optimal control of PEM fuel cells with parametric CMAC networks. *IEEE Trans. Ind. Appl.*, 41:237 – 245, 2005.
- [3] C Bordons, A Arce, and A J DelReal. Constrained predictive control strategies for PEM fuel cells. In *America Control Conference, Minneapolis, USA.*, 2006.
- [4] J K Gruber, C Bordons, and F Dorado. Nonlinear control of the air feed of a fuel cell. In *America Control Conference, Seattle, USA.*, 2008.
- [5] R Talj, M Hilairret, and R Ortega. Second order sliding mode control of the moto-compressor of a PEM fuel cell air feeding system, with experimental validation. In *IEEE Ind. Electronics*, 2009.
- [6] W Gracia-Gabin, F Dorado, and C Bordons. Real time implementation of a sliding mode controller for air supply on a PEM fuel cell. *Journal of Process Control*, 20:325–336, 2010.
- [7] C Kunusch, P F Puleston, M Mayosky, and J Riera. Sliding mode strategy for pem fuel cell stacks breathing control using a super twisting algorithm. *IEEE Transactions on control systems Technology*, 17:167 – 174, 2009.
- [8] J A Moreno and M Osorio. A lyapunov approach to second-order sliding mode controllers and observers. In *47th IEEE Conference on Decision and Control*, Cancun, Mexico, 2008.
- [9] A Levant. Sliding order and sliding accuracy in sliding mode control. *International Journal of Control*, 58:1247–1263, 1993.
- [10] Kyung Won Suh. *Modeling, Analysis and control of Fuel Cell Hybrid Power Systems*. PhD thesis, Department of mechanical engineering, The university of Michigan, 2006.
- [11] R Talj, R Ortega, and M Hilairret. A controller tuning methodology for the air supply system of a pem fuel-cell system with guaranteed stability properties. *International Journal of Control*, Vol. 82, Issue : 9:1706–1719, September 2009.
- [12] J Larminie and A Dicks. *Fuel Cell Systems Explained*. Wiley, New York: 2002.
- [13] CJ Hatziaodoni, A A Lobo, F Pourboghrat, and M Daneshdoost. A simplified dynamic model of grid-connected fuel-cell generators. *Power Delivery, IEEE Transactions on*, 17:467 – 473, 2002.
- [14] S Laghrouche, F Plestan, A Glumineau, and R Boisliveau. Robust second order sliding mode control for a permanent magnet synchronous motor. In *IEEE American Control Conference*, 2003.
- [15] S V Emelyanov, S K Korovin, and A Levant. Higher-order sliding modes in control systems. *Differential Equations*, 29:1627–1647, 1993.
- [16] A Pisano, A Davila, L Fridman, and E Usai. Cascade control of pm dc drives via second order sliding mode technique. *IEEE Trans. Ind. Elec.*, 55, 2008.
- [17] A Levant and L Fridman. Robustness issues of 2-sliding mode control. In *Variable Structure Systems: From Principles to Implementation*, IEE, UK, 129-153, 2004.